Influence of carrier injection on the electromodulation response of trap-rich polymer light-emitting diodes

Cite as: J. Appl. Phys. **99**, 114502 (2006); https://doi.org/10.1063/1.2201692
Submitted: 14 April 2005 . Accepted: 11 April 2006 . Published Online: 01 June 2006

P. J. Brewer, A. J. deMello, J. C. deMello, P. A. Lane, D. D. C. Bradley, R. Fletcher, and J. O'Brien

Influence of carrier injection on the electromodulation response of trap-rich polymer light-emitting diodes

P. J. Brewer, A. J. deMello, and J. C. deMello[a)]
Department of Chemistry, Imperial College London, London SW7 2AZ, United Kingdom

P. A. Lane
Naval Research Laboratory, Washington, DC 20375

D. D. C. Bradley
Blackett Laboratory, Imperial College London, London SW7 2BZ, United Kingdom

R. Fletcher and J. O'Brien
The Dow Chemical Company, Midland, Michigan 48667

(Received 14 April 2005; accepted 11 April 2006; published online 1 June 2006)

We investigate the influence of carrier injection on the electric field distribution in polyfluorene-based polymer light-emitting diodes containing poly(3,4-ethylenedioxythiophene)-poly(styrene sulfonate) (PEDOT:PSS). The devices show strong charge-induced electromodulation spectra due to the accumulation of trapped electrons close to the PEDOT:PSS/polyfluorene interface. The trapped electrons cause the potential to drop preferentially at the interface, enhancing hole injection and substantially reducing the magnitude of the electric field in the bulk semiconductor. The detailed operating mechanisms of such "trap-rich" devices are poorly understood, and in this paper we perform a series of temperature-dependent current-voltage sweeps and electromodulation measurements to clarify the role of the injected charge. We find that the devices show strong field redistribution only at room temperature and that devices operating at lower temperatures (<100 K) resemble trap-free light-emitting diodes with a uniform electric field that extends through the bulk. We consider also the effects of pixel aging and show that field redistribution effects are reduced after extended device operation. © *2006 American Institute of Physics*. [DOI: 10.1063/1.2201692]

INTRODUCTION

Semiconducting polymers are of scientific and commercial interest owing to their applications in optoelectronic devices such as light-emitting diodes, solar cells, and thin-film transistors.[1] There has been significant progress in the development of polymer devices in recent years with, for example, polymer light-emitting diodes (LEDs) now entering the market place as viable contenders to existing display technologies. To some extent, however, attempts to optimize the efficiencies and performance of polymer LEDs have been hindered by the relative absence of detailed models describing device operation. The fundamental processes governing device behavior are the subject of debate and there is considerable interest in experimental measurements that provide insight into device operation.

In earlier studies,[2–5] we used electromodulation (EM) spectroscopy to investigate the strength of the internal electric field in operational polymer light-emitting diodes containing poly(3,4-ethylenedioxythiophene)-poly(styrene sulfonate) (PEDOT:PSS). These measurements indicated that, for many polymer LEDs under light emission conditions, screening effects by injected charge carriers lead to near-complete cancellation of the internal field. In the absence of a sizable bulk field—and hence drift current—carrier transport is mediated primarily by diffusion in a manner similar to light-emitting electrochemical cells.[6] More recently, by fabricating two device types in which the cathode material was selected to provide either efficient (Ba) or inefficient (Al) electron injection, we were able to show that injected electrons trapped close to the PEDOT:PSS/polyfluorene interface are responsible for the field redistribution; in short, only the Ba devices exhibited screening effects indicating that efficient electron injection is a necessary condition to observe screening.[3] The trapped electrons close to the PEDOT:PSS interface cause the potential to drop preferentially at this location, thereby reducing the magnitude of the bulk field. The high field strength at the PEDOT:PSS/polyfluorene interface increases the rate of field-dependent hole injection, leading to improved balance of injection rates for electrons and holes and unexpectedly high device efficiencies. This agrees with independent studies by Murata *et al.*,[7] Woudenbergh *et al.*,[8] and Poplavskyy *et al.*[9] who based on analysis of current-voltage characteristics also found evidence for electron accumulation close to the hole-injecting contact. In this paper, we investigate further how charge injection and trapping influence the operating mechanisms of PEDOT:PSS/polyfluorene-based devices by using the operating temperature as a means of "switching" charge injection on and off.

EXPERIMENTAL OVERVIEW

Devices with an active area of 6 mm^2 were fabricated at The Dow Chemical Company by successively coating an

[a)]Author to whom correspondence should addressed; electronic mail: j.demello@imperial.ac.uk

indium tin oxide (ITO) anode with 80 nm thick layers of poly(3,4-ethylenedioxythiophene)-poly(styrene sulfonate) (PEDOT:PSS) and a fluorene-based light-emitting polymer (LEP), namely, LUMATION (Ref. 10) Green 1300 Series LEP. A 35 nm calcium cathode capped by 150 nm of aluminum was evaporated onto the active layer and the completed device was encapsulated in a nitrogen atmosphere glovebox. The devices were operated in an optically accessible closed-cycle-cooled He cryostat (Oxford Instruments 1100) that permits measurements between 10 and 300 K. EM spectroscopy has been widely used to investigate internal electric fields in organic devices.[11–16] In a typical EM measurement, a combined ac and dc bias $V=V_{dc}+V_{ac}\sin(\omega t)$ is applied to the device and changes in the transmission of a probe beam are monitored using phase sensitive lock-in detection. If the origin of the EM signal is electroabsorption [the Stark effect (SE)], the fractional change in transmission is proportional to the third order dc Kerr nonlinear susceptibility and the square of the electric field.[13] The differential transmission is therefore modulated at both the first and second-harmonic frequencies in accordance with Eqs. (1a) and (1b),

$$I_\omega = \left.\frac{\Delta T}{T}\right|_\omega \propto 2\,\mathrm{Im}\,\chi^3(\lambda)E_{dc}E_{ac}\sin(\omega t), \quad \text{first harmonic}, \tag{1a}$$

$$I_{2\omega} = \left.\frac{\Delta T}{T}\right|_{2\omega} \propto \frac{1}{2}\,\mathrm{Im}\,\chi^3(\lambda)E_{ac}^2\cos(2\omega t), \quad \text{second harmonic}. \tag{1b}$$

Under conditions of low carrier injection, the bulk field E_{dc} is related to the dc component of the applied voltage V_{dc} by $E_{dc}=(V_{dc}-V_{bi})/d$, where V_{bi} is the built-in potential and d is the width of the device. I_ω therefore varies linearly with V_{dc} (passing through zero at $V=V_{bi}$) and $I_{2\omega}$ is independent of V_{dc}; any deviations from this behavior indicate nonuniform internal fields arising from the presence of substantial charge in the device (or, in the case of multilayer devices, contributions from different layers that have distinct spectral characteristics). The measurement of electroabsorption spectra in operational LEDs is complicated by the presence of strong modulated electroluminescence (EL) that is typically several orders of magnitude larger than the EM signal; all measurements reported here were obtained using the double modulation technique of Pires *et al.* permitting the measurement of EM signals as small as one part in 10^7 even for highly emissive operational devices.[17]

RESULTS

In the first series of experiments, measurements were undertaken on "fresh" unused pixels. Figure 1 shows the variation of current density and EL intensity with applied bias at three illustrative temperatures of 300, 150, and 100 K. A delay of 10 s between initial application of the step voltage and each measurement was employed to allow reasonable time for steady state to be achieved. The current-voltage sweeps at 300 and 150 K are symmetric at low biases indicating the presence of small quantities of conducting

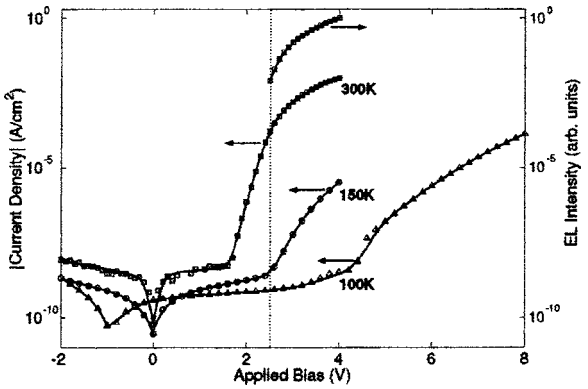

FIG. 1. Current-voltage-luminance measurements for devices based on ITO/PEDOT:PSS/LUMATION Green 1300 Series LEP/Ca/Al. Measurements taken at 300, 150, and 100 K are represented by squares, circles, and triangles, respectively. The symmetrical current-voltage characteristics at low applied bias indicate the presence of conducting filaments in the active layer. The 300 K measurement shows a sharp onset in current at 1.6 V with the onset of electroluminescence occurring at 2.5 V. The current at 150 K is substantially lower and shows a threshold at 2.4 V. The current at 100 K is lower still with a threshold at 4.2 V. No EL is observable at 150 or 100 K over the measurement range.

filaments in the active layer that act as shorts between the electrodes.[18] An interesting feature of the 100 K data is the nonzero minimum in the current-voltage curve. The current should equal zero at an applied bias of 0 V, i.e., when the device is at equilibrium. In fact, for the voltage sweep shown in Fig. 1, the current assumes its lowest value at −1 V. Hysteresis of this nature is generally attributed to the presence of deep electron or hole traps in the semiconductor, which require high time constants to obtain steady state after variation of the applied bias;[19] these time constants are highest at low temperatures due to the slow thermal depopulation of trap states. The room temperature current shows a sharp threshold at ~1.6 V (5.2×10^{-9} A cm^{-2}) with the onset of measurable electroluminescence occurring at 2.5 V (1.6×10^{-4} A cm^{-2}). It will be shown later that 2.5 V corresponds to the built-in potential difference for the device. The current at 150 K is substantially lower due to the reduced (temperature-dependent) carrier mobilities and shows a threshold at 2.4 V (2.5×10^{-9} A cm^{-2}). The current density at 100 K is still lower and shows no obvious threshold until 4.2 V. No EL is observable at 150 or 100 K due to the small currents (and potentially imbalanced nature of the injection) over the measurement range.

Figure 2 shows for a variety of applied biases the first-harmonic electromodulation spectra for the device measured at operating temperatures of 300, 150, and 100 K. In reverse bias, the room temperature spectrum shows a number of features: a broad positive feature at 500 nm, a broad negative feature at 450 nm, a moderately sharp positive feature at 414 nm, and a broad positive feature at 365 nm. These reverse bias features are typical of electroabsorption, an assignment that is confirmed by the observations (not shown) that the spectra scale linearly with the dc bias, quadratically with the ac bias, and are independent of modulation frequency. In forward bias, however, the features beyond 400 nm are largely eliminated, and the broad 365 nm electroabsorption feature is replaced by a strong (and substan-

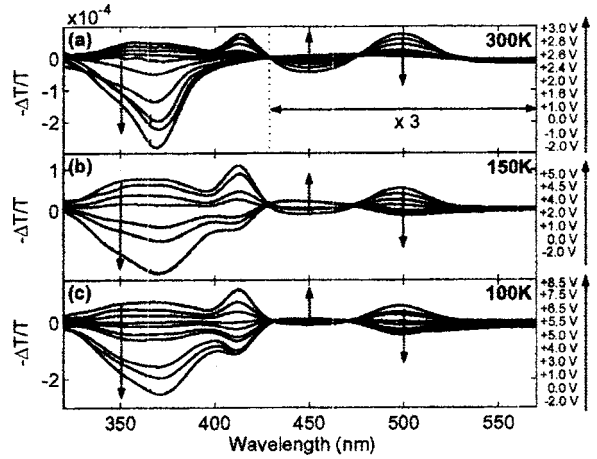

FIG. 2. Electromodulation spectra for an ITO/PEDOT:PSS/LUMATION Green 1300 Series LEP/Ca/Al device obtained at temperatures of (a) 300 K, (b) 150 K, and (c) 100 K. A 167 Hz, 1.0 V rms modulation bias was used to obtain the data in (a) and a 167 Hz, 1.5 V rms alternating bias was employed for (b) and (c). The 300 K spectrum has been magnified by a factor of 3 from 430 to 600 nm for clarity. In reverse bias the spectrum is dominated by the electroabsorption response of the polymer. However, when the device is operating in forward bias, the EA features are replaced by excited state bleaching and absorption due to injected charge. At 150 K the field-induced features identified at room temperature are evident in both reverse and forward biases due to the suppression of charge injection; the charge-induced features do not emerge until 4.0 V. The charge-induced features are further suppressed at 100 K and in this case emerge only above 5.5 V.

tially sharper) negative feature centered at 370 nm. This new feature grows rapidly with applied bias and reaches a maximum at a pixel-dependent bias beyond which it reduces in magnitude (see, e.g., Fig. 3). In a recent paper, we reported that this feature is associated with injected electrons that are localized in trap sites at the PEDOT:PSS/polyfluorene interface.[3] If the assignment is correct, we would expect to "freeze-out" the 370 nm feature at low temperatures [due to

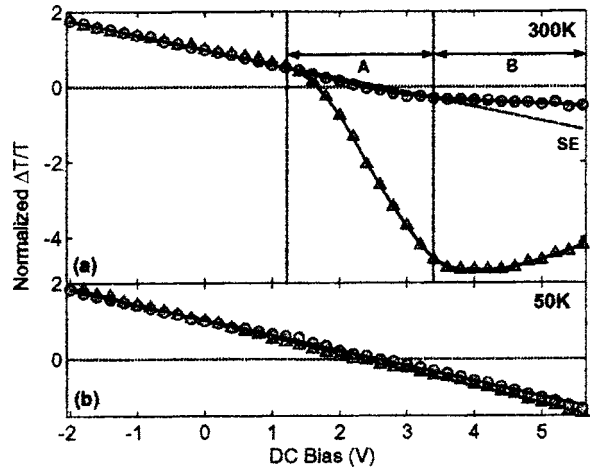

FIG. 3. The normalized dc-bias dependence of the first-harmonic EM signals at 414 and 375 nm. (a) Data obtained at 300 K. The dotted line, labeled "SE," indicates the electroabsorption (Stark effect) response one would expect in the absence of carrier injection. The 414 and 375 nm features, which are denoted by circles and triangles, respectively, overlie one another until 1.2 V at which point charge-induced modulation effects become evident. (b) Equivalent measurements at 50 K, at which temperature charge injection is suppressed. Consequently the 375 and 414 nm signals overlie one another and exhibit Stark effect behavior throughout the bias range.

the reduced current flow in the device (Fig. 1) and hence a reduction in the steady-state trap population] while reintroducing the field-induced features that are absent from the room temperature spectrum. This is indeed the case as may be seen in Fig. 2(b) which shows the EM response at 150 K. The field-induced features identified at room temperature are now present in both reverse and forward biases, and the 370 nm charge-induced feature only emerges at biases above 4 V, at which stage the current again becomes significant. The charge-induced feature is further suppressed at 100 K and, in this case, does not emerge until 5.5 V.

It is informative to examine in more detail the dc-bias dependence of the spectral features identified in Fig. 2. In Fig. 3 we show, for a different pixel on the same substrate, the dc-bias dependence of the first-harmonic signals at 414 nm (circles) and 375 nm (triangles).[20] The 500 and 450 nm electroabsorption features (not shown) exhibited broadly similar behavior to the feature at 414 nm. The data in Fig. 3(a) were obtained at room temperature and have been normalized at 0 V for purposes of comparison. The two normalized signals overlie one another and vary linearly with applied bias in the range $-2 < V < 1.2$ V. However, the 375 nm signal deviates sharply from the linear at +1.2 V. The initial linear response and the subsequent deviation from linearity indicate that up to 1.2 V the main contribution to the 375 nm EM signal is electroabsorption but, beyond this, charge-induced modulation dominates. The magnitude of the 375 nm signal reaches a maximum at +4 V and falls away slowly at higher biases. It is noteworthy that the charge-induced feature due to trapped electrons emerges at a dc bias that is 0.4 V below the current threshold, consistent with the fact that hole injection at the PEDOT:PSS/polyfluorene is highly field dependent and cannot proceed until a large density of electrons have first trapped at the interface. The 375 nm modulation signal actually decreases in magnitude beyond about 4 V, despite the rising current density, and does so in a reversible manner that precludes device degradation as a cause.

The 414 nm data in Fig. 3(a) are intriguing since, although this curve also deviates slightly from the linear at 1.2 V, its gradient dI_ω/dV_{dc} subsequently reduces to zero. This change in slope defines two regimes denoted by A and B on the diagram: in A the signal lies below the dotted "SE-only" line, in B it lies above it. The behavior in regime A is consistent with the 375 nm data, with charge-induced effects leading to an additional negative contribution to the EM signal relative to pure SE modulation. The transition to regime B could potentially be explained by an abrupt phase change in the charge-induced signal, resulting in an overall EM signal of smaller absolute magnitude than SE-only modulation. However, this seems unlikely since there is no evidence of out-of-phase contributions at any wavelength in the forward bias EM spectra of Fig. 2, and any charge-induced contribution at 414 nm is therefore likely to be in phase with the 375 nm main feature, leading to further deviation in the negative direction. Moreover, the 414 nm feature is very nearly independent of the dc bias in regime B, and it is difficult to understand why the field- and charge-induced features should exhibit mirror-image bias dependencies. An al-

ternative explanation which agrees with previous measurements on comparable device structures[2–5] is that, above the turn-on bias of 2.5 V, the injected charges screen the bulk semiconductor from the applied field, thereby suppressing field-induced contributions to the EM signal in regime B. The small near-constant offset from zero in the 414 nm EM signal in regime B is then attributable to a residual charge-induced contribution that is in phase with the main 375 nm feature. We note that, in measurements on previously reported devices, we were able to identify spectral regions in which the electroabsorption signal was uncontaminated by charge-induced modulation, and at these wavelengths full extinction of the EM signal was observed when screening occurs. In the present case, however, it was not possible to find a spectral region which had a sufficiently intense electroabsorption response to obtain a decent signal but that did not also have some contamination from charge-induced modulation—hence the small offset observed at 414 nm in regime B.

In Fig. 3(b), we show the bias dependencies of the 375 and 414 nm features at 50 K, at which temperature the rates of carrier injection from the electrodes are low and therefore we expect little if any charge-induced modulation. The two (normalized) EM signals overlie one another closely and vary linearly with applied bias over the full measurement range in agreement with Eq. (1a). Their slopes match closely with the linear regions of the room temperature curves in Fig. 3(a), which provides further confirmation that the room temperature signals in the range $-2 < V < 1.2$ V are indeed field induced. The built-in potential difference may be determined from the intersection of these lines with the x axis, which yields an approximate value of 2.5 V. The same approximate value is obtained by extrapolating the linear regions of the signals in Fig. 3(a) to the x axis. The 375 nm signal at 50 K is the marginally steeper of the two curves due to a small amount of charge-induced modulation even at 50 K which is more significant at 375 nm. The 414 nm feature remains linear over the full measurement range at 50 K and does not show the reduction in slope observed at 300 K, indicating that the room temperature behavior is indeed related to the injection of charge as argued above.

The room temperature measurements described above were repeated using an "aged" pixel that had previously been operated continuously for 217 h under dc bias at room temperature. The device was driven to half luminance under constant current conditions (11 mA/cm^2) from an initial luminance of 1000 cd/m^2. Device efficiencies before and after aging were 9.1 cd/A (7.3 lm/W) and 4.5 cd/A (2.9 lm/W), respectively. Figure 4(a) shows the current-voltage-luminance characteristics of the aged pixel. The current-voltage characteristics below turn on are again highly symmetric but the current in this regime has increased by a factor of 10 relative to the unaged pixel, indicating the formation of additional conducting filaments. In consequence, the current threshold—which indicates the point at which conduction via the semiconductor becomes competitive with filamentary conduction—is delayed until 2 V. Figure 4(b) shows the first-harmonic electromodulation spectrum for the aged pixel; it has a broad feature that extends to very short wavelengths (below 300 nm) and appears to overlap with the 370 nm charge-induced modulation feature observed in the unaged pixel (although it might equally correspond to a broadening of the 365 nm peak). The emergence of this new/altered charge-induced feature indicates that a chemical or physical change in the active layer has taken place following extended operation. It is not yet clear whether there is a causal link between this change and the increase in filament density but the presence of filaments is generally considered to accelerate device degradation through localized Joule heating effects.[18] Figure 4(c) shows the dc-bias dependence of the first-harmonic signal at 375 and 414 nm. The two signals vary linearly with applied bias in the range $-2 < V < 1$ V but the 375 nm signal deviates sharply from the linear at 1 V in the negative direction and increases in magnitude over the full measurement range up to 6 V. This is different from the behavior in the fresh pixel for which the charge-induced feature was found to diminish reversibly at 4 V. The 414 nm feature maintains its linear trend until 3 V at which point the slope reduces slightly. The inset compares the bias dependence of the 414 nm feature in the fresh and aged pixels and indicates that the initial deviation in the negative direction is smaller for the aged pixel. In addition, although (as with the unaged pixel) the 414 nm signal subsequently crosses above the SE-only line, its gradient does not reduce to zero, indicating a much weaker degree of field screening in aged pixels.

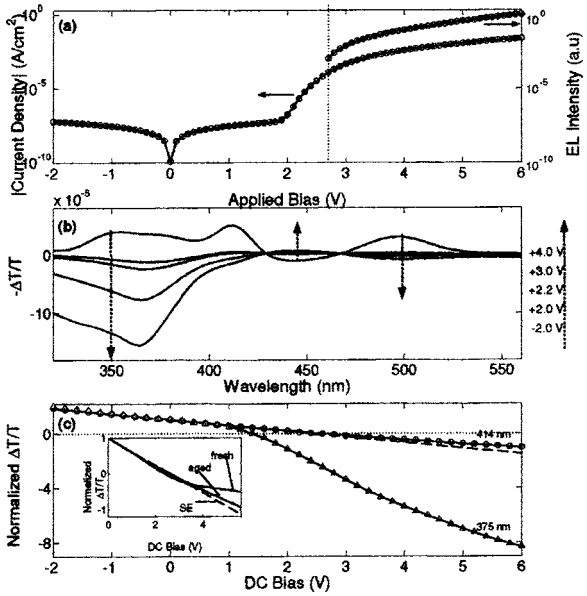

FIG. 4. Experimental measurements for an aged pixel: the device was run continuously for 217 h under dc bias (constant current ≈11 mA/cm^2), causing the luminance to drop to half of its initial 1000 cd/m^2 value. (a) The current-voltage-luminance characteristics. (b) First-harmonic electromodulation spectra for a variety of applied biases. (c) The dc-bias dependence of the first-harmonic signal at 375 and 414 nm (triangle and circle data points, respectively). The inset compares the bias dependence of the 414 nm feature in a fresh pixel and the aged pixel. The weak deviation from linearity (dashed lined) above turn on in the aged pixel indicates a much weaker degree of field screening.

CONCLUSION

In conclusion, we have investigated the effects of temperature and extended operation on polymer LEDs contain-

ing PEDOT:PSS. The EM spectra of these devices may be explained in terms of field- and charge-induced features. The room temperature EM spectra are dominated by field-induced features in reverse bias and charge-induced features in forward bias: By selecting a wavelength (414 nm) at which the electroabsorption response was strong, we were able to show suppression of the field-induced features above turn on, consistent with field screening due to trapped electrons at the PEDOT:PSS/polyfluorene interface. The charge-induced features may be eliminated by reducing the temperature of the device in order to lower the circulating current. This results in a conventional electroabsorption response in both forward and reverse biases, with no evidence of field redistribution. The profile of the charge-induced features is modified after extended operation, indicating physical or chemical changes in the active layer. These changes are accompanied by a reduction in the observed degree of field screening.

ACKNOWLEDGMENTS

We are grateful for financial support from the UK Engineering and Physical Sciences Research Council and to The Dow Chemical Company for the provision of the light-emitting diodes used in this work.

[1]R. H. Friend *et al.*, Nature (London) **397**, 121 (1999).
[2]P. J. Brewer, P. A. Lane, A. J. deMello, D. D. C. Bradley, and J. C. deMello, Adv. Funct. Mater. **14**, 562 (2004).
[3]P. J. Brewer, P. A. Lane, J. Huang, A. J. deMello, D. D. C. Bradley, and J. C. deMello, Phys. Rev. B **71**, 205209 (2005).
[4]P. A. Lane, J. C. deMello, R. B. Fletcher, and M. Bernius, Appl. Phys. Lett. **83**, 3611 (2003).
[5]P. A. Lane, J. C. deMello, R. B. Fletcher, and M. T. Bernius, Proc. SPIE **5214**, 162 (2004).
[6]J. C. deMello, N. Tessler, S. C. Graham, and R. H. Friend, Phys. Rev. B **57**, 12951 (1998).
[7]K. Murata, S. Cina, and N. C. Greenham, Appl. Phys. Lett. **79**, 1193 (2001).
[8]T. v. Woudenbergh, P. W. M. Blom, and J. N. Huiberts, Appl. Phys. Lett. **82**, 985 (2003).
[9]D. Poplavskyy, J. Nelson, and D. D. C. Bradley, Appl. Phys. Lett. **83**, 707 (2003).
[10]Trademark of The Dow Chemical Company.
[11]J. C. deMello, J. J. M. Halls, S. C. Graham, N. Tessler, and R. H. Friend, Phys. Rev. Lett. **85**, 421 (2000).
[12]C. Giebeler *et al.*, Appl. Phys. Lett. **74**, 3714 (1999).
[13]I. H. Campbell, T. W. Hagler, D. L. Smith, and J. P. Ferraris, Phys. Rev. Lett. **76**, 1900 (1996).
[14]P. A. Lane, J. Rostalski, C. Giebeler, S. J. Martin, D. D. C. Bradley, and D. Meissner, Sol. Energy Mater. Sol. Cells **63**, 3 (2000).
[15]S. J. Martin, G. L. B. Verschoor, M. A. Webster, and A. B. Walker, Org. Electron. **3**, 129 (2002).
[16]I. Hiromitsu, Y. Murakami, and T. Ito, J. Appl. Phys. **94**, 2434 (2003).
[17]M. P. Pires, P. L. Souza, and J. P. V. d. Weid, Braz. J. Phys. **26**, 252 (1996).
[18]R. G. Sharpe and R. E. Palmer, J. Phys.: Condens. Matter **8**, 329 (1996).
[19]W. Brutting, H. Riel, T. Beierlein, and W. Riess, J. Appl. Phys. **89**, 1704 (2001).
[20]It should be noted that, although the maximum in the charge-induced feature lies at 370 nm, the absolute values of T and ΔT are largest at 375 nm. The dc-bias dependence of the charge-induced feature was therefore obtained at this wavelength instead.